CMD 2026 Conference
The 3rd International Online Conference on Corrosion and Materials Degradation
In Memoriam of Prof. Dr. Digby Macdonald
30 June – 2 July 2026 Online
MDPI

Atmospheric corrosivity in a bagasse/coal co-firing power plant influenced by a tropical marine climate

Yashwantraj Seechurn
Mechanical and Production Engineering Department, Faculty of Engineering, University of Mauritius, Reduit 80837, Mauritius

INTRODUCTION & AIM

Outdoor steel infrastructure corrodes when subjected to conditions governed by the temperature-humidity complex, airborne chloride (Cl^-), oxygen diffusion, contaminants like sulphur dioxide (SO_2), and anthropogenic particulates. Following field exposure of carbon steel at various locations countrywide, a corrosion map for Mauritius had been developed. However, the previous investigations exclude marine-industrial regions with favourable wind patterns. This study provides valuable information on the corrosion mechanism at such a unique location and concurrently helps validate the corrosion map.

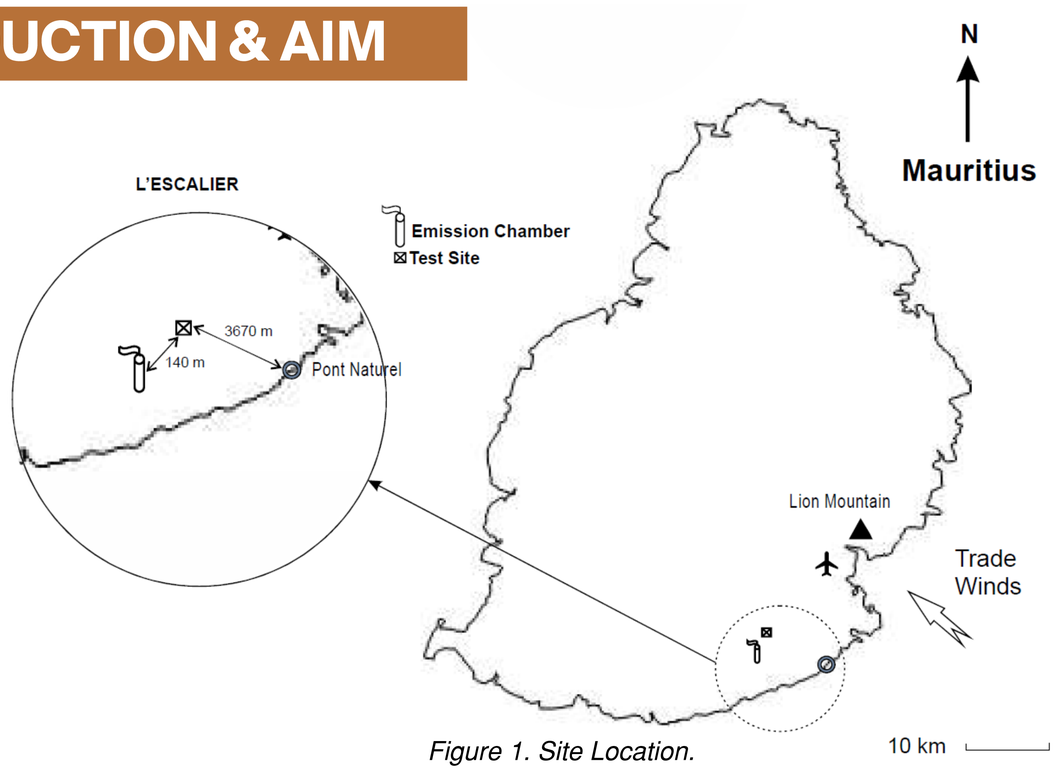

Figure 1. Site Location.

Table 1. Chemical Composition of S235 grade carbon steel (%Wt)

C	Mn	P	S	Si	Ni	Cu	Fe	Cr	Mo
0.26	0.75	0.04	0.05	0.004	0.012	0.55	98.3	-	-

METHOD

To determine the atmospheric corrosivity, bare S235 grade carbon steel (CS) plates of the composition shown in Table 1 and dimensions $150\,mm \times 100\,mm \times 3\,mm$ were exposed for a period of 14 months at L'Escalier, about 3.67 km from the seacoast and 0.14 km from the emission chambers of a bagasse/coal thermal power plant (*Fig. 1*). The 45° exposure rack was placed downwind and aligned with prevailing wind directions, at an elevation of 98 m above sea level, facing the ocean (*Fig. 2*) [1]. Mass loss and surface analysis (using FTIR and SEM/EDS) were performed on corroded specimens removed at specific timepoints.

Figure 2. Exposure of bare CS specimens for a period of 14 months.

RESULTS & DISCUSSION

According to ISO 9223, L'Escalier falls in the S_2 category (60 $mgm^{-2}d^{-1}$ < S < 300 $mgm^{-2}d^{-1}$) and SO_2 falls in the P_1 category (4 $mgm^{-2}d^{-1}$ < P ≤ 24 $mgm^{-2}d^{-1}$). The Time of Wetness (TOW) was calculated to be around 1926 ha^{-1} (τ3). The one-year corrosion rate (r_{corr}) obtained from mass loss analysis indicate an atmosphere of C3 category i.e., medium corrosivity. *Fig. 3* shows a graph of *D* (gm^{-2}) vs. t (*a*).

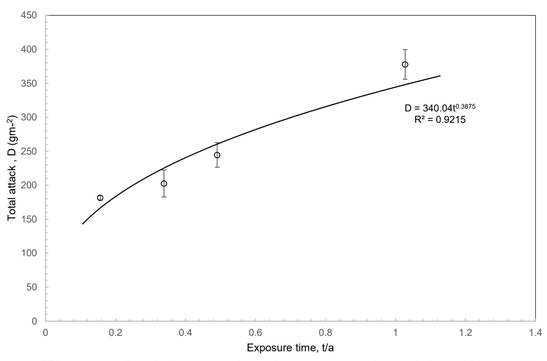

Figure 3. Atmospheric corrosion kinetics of carbon steel in L'Escalier (marine-industrial).

The corrosion rate followed the bi-logarithmic equation, $D = r_{corr}t^b$, with an attenuating r_{corr} due to the accumulation of corrosion products at the metal surface. A '*b*' value of 0.4 indicates that the corrosion products eventually form an effective barrier between the electrolyte and the metal substrate. However, the initial high corrosion rate suggests that the rust layers formed in the early stages are porous, thus allowing ingress of aggressive species.

FTIR analysis shows that the samples exposed for two, four, and six months revealed the consistent presence of lepidocrocite (γ-FeOOH) with strong peaks around 1020 cm^{-1} and 450 cm^{-1} [3,4] (*Fig.4*). Thus, indicating that the corrosion process was still taking place due to the porous nature of γ-FeOOH. Goethite (α-FeOOH) was found with peaks at 798 cm^{-1} and 880 cm^{-1} at two months [4]. Additionally, successive peaks around 1644 cm^{-1} from two to six months confirmed the predominance of this compact and adherent layer [5], which explains the decrease in corrosion rate observed by the mass loss method.

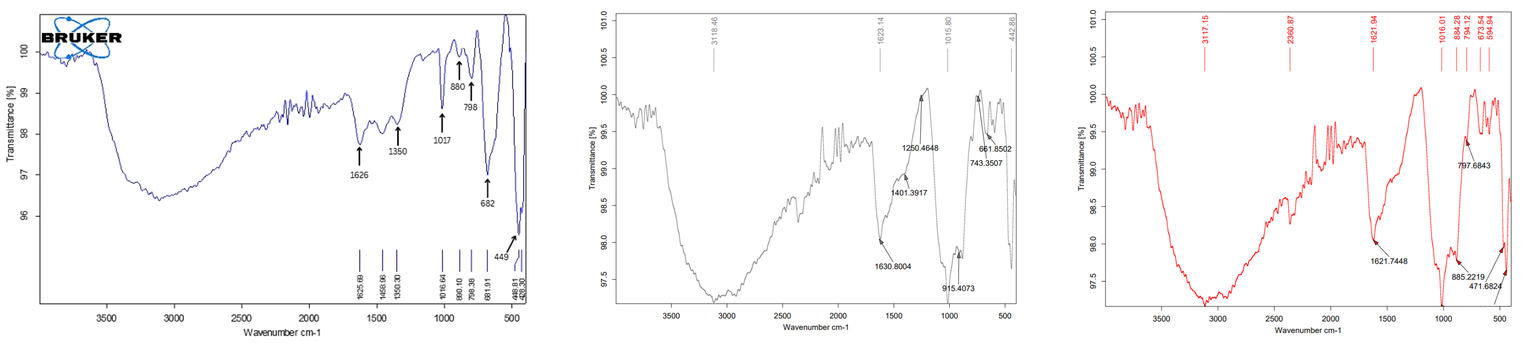

Figure 4. FTIR spectra of rusts scraped off the surface of carbon steel exposed for two months (left), four months (middle), and six months. (right).

Crystalline sandy crystals and globular cotton ball formations (*Fig. 5*) are attributed to the presence of γ-FeOOH and α-FeOOH, respectively. α-FeOOH is mainly formed in the presence of SO_2, as can be seen in the EDS spectra (*Fig. 6*), which confirms the presence of sulphur. The absence of magnetite (Fe_2O_3) indicates oxygen deficiency at the interface. Therefore, it is the existing rust phase that oxidizes, resulting in more α-FeOOH formation.

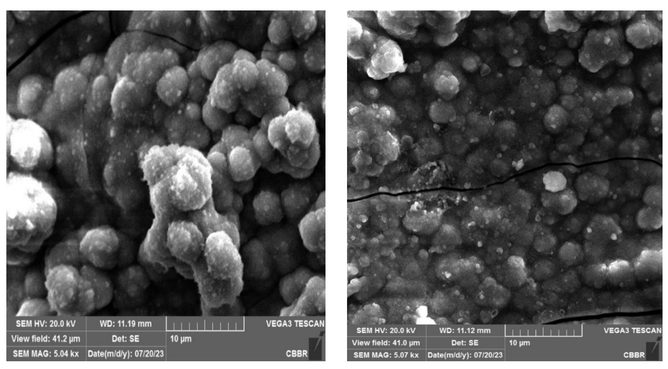

Figure 5. SEM images showing globular cotton balls (left) and crystalline sandy crystals (right) on carbon steel exposed for six months.

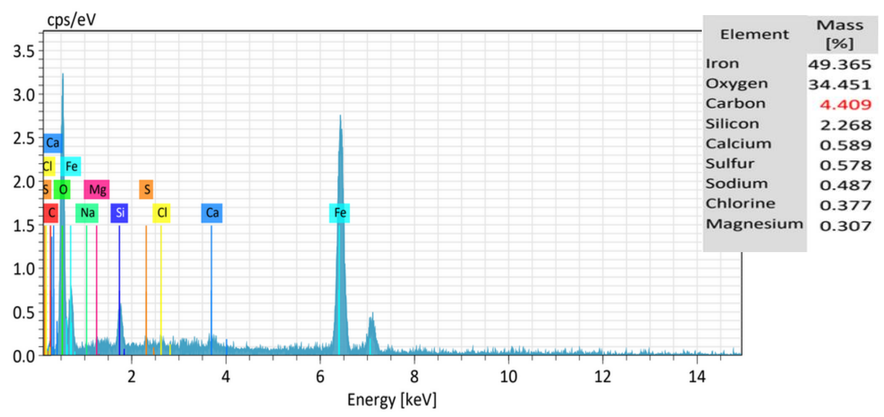

Figure 6. EDS spectrum of carbon steel exposed for six months.

CONCLUSIONS

- The Cl^- deposition rate, although in the S_2 category, doesn't reach the threshold for the formation of flaky corrosion layers, which would indicate the presence of the akaganeite (β-FeOOH) rust phase.
- SO_2 emissions do not lead to significant surface deposition. Wind patterns and stack height should be considered in categorizing the aggressivity of an atmosphere.
- The corrosion progression follows the expected power law trend with an exponent value of 0.4, implying adequate protective ability of the rust layer under the attack of aggressive species.
- Extreme corrosion protection measures may not be required in power plants.

ACKNOWLEDGEMENTS

The author acknowledges Dheeresh Singh Goorbine for his contribution in the field exposure and data collection phases of this study.

REFERENCES

[1] ISO 8565, Metals and alloys - Atmospheric corrosion testing: General requirements, 2011.
[2] BS EN ISO 9223, Standards Publication Corrosion of metals and alloys- Corrosivity of atmospheres - Classification, determination and estimation, 2012.
[3] M. Jia, P. Hu, G. Hu, Corrosion Layers on Archaeological Cast Iron from Nanhai I, Materials 15 (2022) 4980. https://doi.org/10.3390/ma15144980.
[4] M. Veneranda, J. Aramendia, L. Bellot-Gurlet, P. Colomban, K. Castro, J.M. Madariaga, FTIR spectroscopic semi- quantification of iron phases: A new method to evaluate the protection ability index (PAI) of archaeological artefacts corrosion systems, Corros. Sci. 133 (2018) 68–77. https://doi.org/10.1016/j.corsci.2018.01.016.
[5] N. H. Dahon *et al.*, "FTIR Analysis on Phase Transformation of Rust In The Presence of Gambir," *Journal of Global Scientific Research*, vol. 1, pp. 54–62, 2018, [Online]. Available: www.gsj-pub.comwww.gsj-pub.com/JGSR